Performance of an Optical Pyramidal Fly-eye Diversity Receiver for Indoor Wireless Communication Systems in the Presence of Background Noise and Multipath Dispersion

A. G. Al-Ghamdi and J. M. H. Elmirghani

University of Wales Swansea

Abstract: An investigation into the optical wireless system performance has been carried out for both a conventional hybrid system (CHS) with a single detector under various receiver fields-of-view (FOV) and a pyramidal fly-eye diversity receiver (PFDR) with different FOVs. Original results for a hybrid system that employs a PFDR, under different FOVs, are presented. It is demonstrated, through FOV optimisation of both the CHS and the PFDR, that the CHS performance is more severely affected by background noise and multipath dispersion than a PFDR system. Furthermore, SNR results are presented demonstrating that our optimised PFDR antenna gives about 4 dB improvements over the CHS. It is also demonstrated that the pulse spread induced by the multipath dispersion is significantly reduced when the PFDR receiver FOV is set to its optimum value.

1 Introduction.

In the last few years, an enormous growth in data communication for indoor and outdoor applications has been witnessed. These applications have been established using both wired physical connections and wireless systems. Physical connections present difficulties in reconfiguring, maintaining, and rewiring wired networks. However, in general, the cabling problem ranges from low cost loose wire solutions on the floor to very high cost crowded ducts. On the other hand, the great aim of faster, flexible, inexpensive, and high-speed data communication, for portable network devices in work and living environments, has prompted great attention for infrared wireless systems. The OW system is not without drawbacks, however. In indoor infrared applications, distortion due to multipath dispersion can cause system degradation [1]. Furthermore, ambient light arising from sunlight, fluorescent, and incandescent lighting induces background noise (BN) in optical wireless receivers. Moreover, the transmitter power is constrained by eye and skin safety regulations [2]. A possible technique that can be used to reduce multipath dispersion, background noise, and shadowing caused by obstacles, as well as to improve the received signal power, is diversity detection [3]. Improvement in performance can be achieved by using a number of uncorrelated narrow FOV receivers rather than a single wide FOV receiver.

2. Propagation environment

End-to-end signal propagation is not only effected by the channel, but also the transmitter and receiver beams and radiation/reception patterns. In order to examine the effects of multipath dispersion and ambient light noise and their impact on the received data stream in indoor wireless applications, propagation simulations were conducted in a rectangular room. Signal propagation between transmitter and receiver is considered to be confined within a room whose dimensions are 8m $\times$ 4m $\times$ 3m. Walls (including ceiling) and floor are modelled as Lambertian reflectors of the first order with reflectivity's coefficients 0.8 and 0.3, respectively. Reflections from doors and windows are considered completely the same as reflections from walls. The transmitter is placed in the middle of the ceiling where it emits 0.4 W as an ideal Lambertian radiation towards (normal to) the communication floor (CF), a surface 1m above the floor where the receiver is placed. Safety standards have been established for laser safety in which optical transmitters are classified in accordance with the total transmitted power [2]. Optical radiation at such amount of power can present a hazard to the eye and to the skin. In spite of that, different techniques can be used to reduce the impact of high laser power such as holograms mounted on the transmitter or the use of arrays of transmitters [5]. The receiver is assumed to have a photodiode with an active area (A_r) of 1 cm^2. An optical concentrator similar to the one used in [1] was adopted. To facilitate the characterisation of the communication environment, the receiver was placed in different locations on the CF.

The transmitter can be modelled using a Lambertian law. The angular distribution of the transmitter radiant intensity (W/str) is given by [1]

$$dp_n = \frac{n+1}{2\pi} \times P_s \times cos^n(\vartheta_i), \tag{1}$$

where P_s is the total average transmitted optical power radiated by the LED source, ϑ_i is the emission angle with respect to the transmitter's surface normal, and n is the mode number describing the shape of the transmitted beam. In order to compute the received signal power for a conventional hybrid channel that employs a single detector, the test room's walls and ceiling have been divided into equal square reflection elements with a dA of 20cm $\times$ 20cm. The reflection elements were treated as small emitters that diffuse the received signal from their centres in the form of a Lambertian pattern. The average signal power reflected by a wall and detected by the detector can be written as

$$dp_r = \frac{n+1}{2\pi^2 R_1^2 R_2^2} P_s \times A_r \times \rho \times cos^n(\vartheta_i) \times cos(\beta) \times cos(\gamma) \times cos(\delta) \times dA \times rect(\delta / FOV), \qquad (2)$$

where *r* is the reflection coefficient at the surface element, **b** is the angle between the direction of the ray and the normal to the surface element, γ is the angle between the reflected ray and the normal of dA, **d** is the angle between the surface normal of the detector and the incident ray, R_1 is the distance between the transmitter and the dA, and R_2 is the distance between the surface element and the detector. The step function *rect(d/FOV)* describes the relationship between the FOV of the photodetector and the received angle. Changing the receiver's FOV can be used to reject unwanted light, since, the signal must lie within the FOV range of angles to be received.

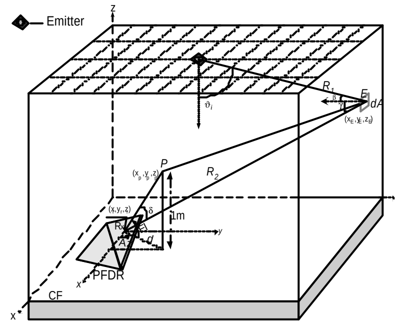

Figure 1: Power analysis model for a PFDR configuration.

On the other hand, the proposed PFDR receiver was reported in [4], with three photodetectors each placed at the middle of a pyramid's face, where the centre of the pyramid's triangular base plane specifies the location of the PFDR receiver on the CF. The direction of each photodetector is characterised by two major parameters: elevation angle (*El*) and orientation angle (azimuth angle *Az*). The other parameters of interest include the pyramid's face inclination and the size of the pyramid. While the *El* angle remains 30^o for all photodetectors, the *Az* angle corresponds to the pyramid's face orientation angles, which are fixed to 15^o, 135^o, and 255^o. Compared with the CHS analysis where the vector normal to the receiver is also perpendicular to the CF, changes in the calculations for the received power analysis need to be made in the case of the PFDR. The reception angle can be calculated by employing the trigonometry of rectangular triangles as shown in Fig. 1. The power received due to an element *dA* in the case of using a PFDR is obtained as

$$dp_r = \frac{n+1}{2\pi^2 R_1^2 R_2^2} P_s \times A_r \times \rho \times cos^n(\vartheta_i) \times cos(ß) \times cos(?) \times \left[\frac{\left|\overrightarrow{PR_x}\right|^2 + \left|\overrightarrow{ER_x}\right|^2 - \left|\overrightarrow{EP}\right|^2}{2\left|\overrightarrow{PR_x}\right|\left|\overrightarrow{ER_x}\right|} \right] \times rect(d/FOV)dA \qquad (3)$$

where the vectors $\overrightarrow{PR_x}, \overrightarrow{ER_x}$, and $\overrightarrow{EP}$ are as shown in Fig. 1.

3. System performance in an ambient noise interference environment

In this section, the SNR of the OW system is analysed in a very directive noise environment. The performance achieved by the PFDR at various FOVs is compared with the performance of the CHS system.

3.1 Ambient light

The major sources of ambient light in an indoor environment include daylight, incandescent light, for example halogen and tungsten filament lamps, and fluorescent light sources. These sources emit a substantial amount of power within the wavelength range of silicon photodetectors as well as introducing shot noise and can saturate the photodetector when their intensity is high [6]. Although ambient light can be much stronger than the transmitted data signal, certain measures (such as optical filters) can be used to minimise its influence.

It has been shown that ambient light, such as an incandescent lamp illumination, can be modelled as a Lambertian source [7]. Therefore the background light level (background noise BN) at the receiver produced by such a source can be written as:

$$P_n = P_{nd} + \frac{n+1}{2\pi^2 R_1^2 R_2^2} \times P_l \times A_r \times \rho \times \cos^n(\vartheta_i) \times \cos(\beta) \times \cos(\gamma) \times \cos(\delta) \times dA \times rect(\delta / FOV), \qquad (4)$$

where P_l is the optical power emitted by the light source and P_{nd} is the direct path component of the BN.

In order to assess the system's performance as well as examine the advantages of having a diversity detection receiver, eight halogen spotlights, which result in one of the most stringent optical spectral corruption to the received data stream, have been chosen. To evaluate the impact of ambient light, the BN distribution pattern of an incandescent light was investigated. 'Philips PAR 38 Economic' (PAR38) was investigated. PAR38 emits a power of about 65 W in a narrow beamwidth with n= 33.1. The eight spotlights were placed 2 m above the CF at the locations shown in Fig. 2. These lamps produced a well-illuminated environment and three photodetectors were placed on the pyramid's faces. Simulation of the optical noise power along both axes of CF was carried out in steps of 10 cm.

The results show that optimising the PFDR FOV to a FOV of 120^o reduces the peak BN level by a factor of 2 compared to the CHS; no optical filter was used in both cases. Table 1 illustrates the background noise level for different FOVs at the worst position on the CF (under a spotlight).

It should be noted that in the case of the PFDR when the FOV is reduced to a value less than 120^o, the background noise is reduced gradually until a certain FOV is reached (60^o), at which point a significant reduction in BN can be observed. At a FOV= 60^o the direct LOS component is lost between the spotlights and the receiver, almost at all points on the CF when a PFDR is used. Note that the data transmitter has n= 1 and thus has a wide beam which enables the PFDR to simultaneously maintain LOS for signal and loose LOS for noise. LOS with noise sources (spotlights) is lost since these are more directive (n= 33.1) than the data transmitter. This observation is key to our proposed scheme. Clearly, the findings indicate that the PFDR can loose the LOS component to a spotlight if FOV is reduced. Most of the BN power is contributed by the LOS component when the influencing source is directive. A FOV= 60^o, however, results in a high delay spread as shown in Fig. 3.

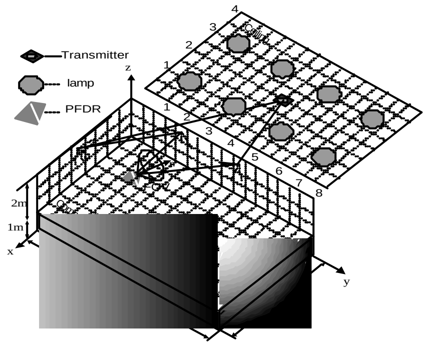

Figure 2: Eight spotlights distribution in a PFDR configuration.

3.2 Signal-to-noise ratio calculations

To evaluate the effect of reducing the receiver FOV on the system performance, we first need to classify noises that disrupt the received data stream at the point of reception. Noise in these systems can be classified into three categories: background shot noise (s_{bn}), noise associated with the incident signal power (s_s) and noise associated with the optoelectronic receiver (s_{pr}). Background noise level can be evaluated by computing the corresponding shot noise current. The noise induced by the received signal power which consists of two components: shot noise current (s_{s1}) when a '1' is received and shot noise current (s_{so}) when a '0' is received. This signal dependent noise is very small in this case and can be neglected. The receiver noise is generated in the preamplifier components. The preamplifier used in this study is the PIN-BJT design proposed by Elmirghani *et al.* [8]. This preamplifier has a noise current density of 2.7 $pA/\sqrt{Hz}$ and a bandwidth of 70 MHz, therefore the preamplifier shot noise is given by

Configuration	FOV	Maximum BN (μW)	*Peak BN shot noise current (s_{bn}), (μA)*	Maximum Delay spread (ns)
PFDR	180^o	4500	0.23	1.33
	120^o	4500	0.23	1.2
	60^o	41	0.0022	3.1
CHS	180^o	9000	0.31	2.3
	120^o	9000	0.31	4.68

Table 1: Maximum BN evaluated under a spotlight (n=33.1) and maximum delay spread evaluated over the entire CF.

$$s_{pr} = (2.7)\times 10^{-12}\times \sqrt{70\times 10^6} = 0.023\ \mu\text{A}.$$

Background noise was evaluated for a typical ambient light source (very directed source n= 33.1) and under various PFDR FOV values. The resultant shot noise current values s_{bn} are given in Table 1. Calculations were based on the worst case where P_{bn} is at its peak. In order to evaluate the system performance, the received pulse shapes for both configurations (PFDR and CHS) have been considered in calculating P_{s1} and P_{s0}, the power associated with logic 0 and logic 1 respectively. The SNR taking P_{s1} and P_{s0} into account (hence ISI) is

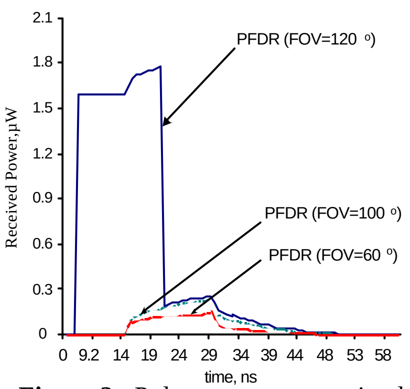

Figure 3: Pulse responses received by CHS and PFDR receiver, at x= 2m, y=4m.

$$SNR = Q^2 = \left(\frac{R\times\left(P_{s1} - P_{s0}\right)}{\sqrt{\sigma_{pr}^2 + \sigma_{bn}^2 + \sigma_{s0}^2} + \sqrt{\sigma_{pr}^2 + \sigma_{bn}^2 + \sigma_{s1}^2}} \right)^2, \qquad (5)$$

where Q is the Gaussian function, which assumes a value of 6 at probability of error $P_e = 10^{-9}$, R = 0.5A/W is the photodetector responsivity, and σ_{s0} and σ_{s1} are the shot noise currents associated with P_{s0} and P_{s1} respectively.

SNR calculations were performed for both systems in seven different locations along the y-axis at constant x= 2m and x= 3m, where x= 3m scans the peaks and troughs of BN and x= 2m corresponds to low BN values in most cases as shown in Fig. 4. Fig. 4 also shows the *SNR* for both the PFDR and CHS at two FOVs (180^o and 120^o). Comparing the results shown in those figures, it can be seen that, in spite of employing different types of receivers, the signal degradation is clearly visible at locations near the wall sides and the room corners as the difference in distance between the transmitter and the receiver increases and the emitter illuminations decrease.

In contrast, a remarkable improvement in the *SNR* is seen, in particular at these weakest points when a PFDR with a FOV= 120^o is used (Fig. 4). In view of the fact that the weakest points in a communication link is the criterion of the system quality, the minimum *SNR*s of the two configurations (PFDR and CHS) have been compared. These are 26.2 dB and 9.8 dB for the CHS with FOV=180^o, at (2m, 0.5m) and (3m, 1m), respectively, and 30 dB and 15 dB for the PFDR configuration at the two locations, see Fig. 4. The improvement obtained by using the latter structure can be seen; more than 4 dB improvement over the CHS configuration.

It can be clearly seen that the PFDR with a FOV=120^o results in the lowest delay spread accompanied by a reasonable *SNR* that can achieve a probability of error of about 10^{-9} at the worst locations. The reduction in delay spread and the good *SNR* are major advantages of the PFDR configuration over the conventional hybrid configuration over the entire CF.

Despite the distorted pulse shape, at the PFDR FOV of 60^o, where the LOS component vanishes, it is found that this configuration offers a good *SNR* over the entire CF as shown in Fig. 5. This remarkable improvement in the *SNR* is attributed to the fact that the maximum level of BN, at n= 33.1, for the PFDR system has dropped from 4.6 mW when the PFDR has a FOV= 120^o to 41 µW when FOV= 60^o. Moreover, the r.m.s background shot noise current has greatly dropped from 0.23 µA at FOV=120^o to 0.022 µA at FOV=60^o, which is a value comparable to the preamplifier noise. The results in Table 1 were based on the worst case where P_{bn} is at its peak. Therefore, selecting either a PFDR with FOV=120^o or 60^o is dictated by the application and the magnitude of the background noise. FOV= 60^o is good when the delay spread is not a concern (lower bit rates), while FOV=120^o is good when ISI is an issue.

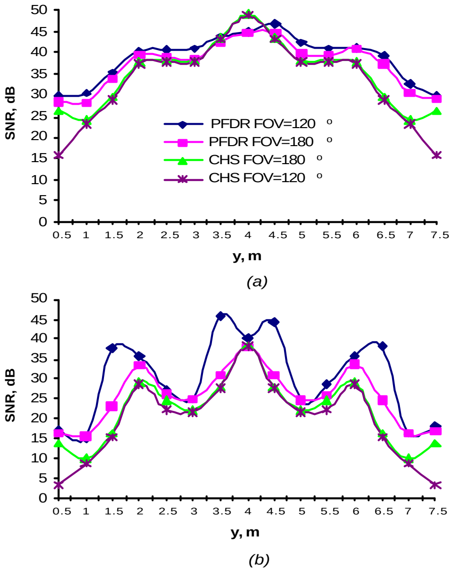

Figure 4: Signal-to-noise ratio level for PFDR and CHS; (a) x= 2m; (b) x= 3m along the y-axis.

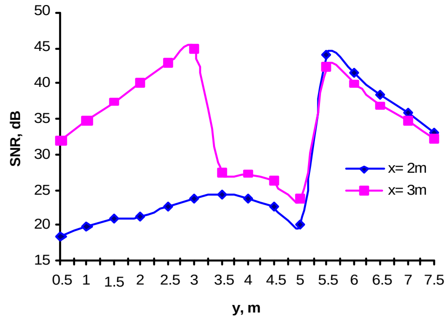

Figure 5: Signal-to-noise ratio level for PFDR with FOV=60^o.

4. Conclusions

The FOV of a PFDR system was optimised and it was shown that optimising the FOV of such a system could lead to a significant performance improvement. It was also shown that a very narrow FOV leads to a significant pulse spread (and background noise reduction) and hence an optimum FOV exists. Comparison with the single detector hybrid system has shown that the PFDR at FOV= 120^o can increase *SNR* from 9.8 dB to 15 dB in the worst case (i.e. underneath a spotlight along x= 3m line). Consistently better performance was obtained throughout the room geometry with the PFDR but not with the conventional hybrid system.

5. References

[1] J. M. Kahn and J.R.Barry, "Wireless infrared communications," *Proc. Of the IEEE*, pp.265-298, Feb. 1997.

[2] "Optical Radiation Safety and Laser Equipment". IEC 60825-1 amendment 2, 2001.

[3] C. R. A. T. Lomba, R. T Valadas, and A. M. De Oliveira Duarte, "Sectored receivers to combat the multipath dispersion of the indoor optical channel," PIMRC'95, Toronto, Canada, pp. 321-325, 1995.

[4] K. L. Sterckx, J. M. H. Elmirghani, and R. A. Cryan, "Pyramidal Fly-eye Detection Antenna for Optical Wireless Systems," *IEE Colloq. Opt. Wirel. Commun.*, London, UK, pp. 5/1-5/6, June 1999.

[5] Svetla T. Jivkova and Mohsen Kavehrad, "Multispot diffusing configuration for wireless infrared access," *IEEE Trans. on commun.*, vol. 48, no. 6, pp. 970-978, June 2000.

[6] A. J. C Moreira, R. T. Valadas, and A. M. de Oliveira Duarte, " Optical interference produced by artificial light," *Wireless Networks*, vol.3, pp. 131-140, 1997.

[7] H. H. Chan, K. L. Sterckx, and J. M. H. Elmirghani, "Performance of optical wireless OOK and PPM systems under the constraints of ambient noise and multipath dispersion," *IEE Comm. Magazine*, vol. 36, no.12, pp.83-87, December 1998.

[8] J. M. H. Elmirghani, H. H. Chan, and R. A. Cryan, "Sensitivity evaluation of optical wireless PPM systems utilising PIN-BJT receivers," *IEE Proc. Optoelectron*,, vol. 143, no. 6, pp. 355-359, December 1996.